Phys. Status Solidi B **250**, No. 10, 2158–2162 (2013) / **DOI** 10.1002/pssb.201350013

physica status solidi b
www.pss-b.com
basic solid state physics

Competing A-site and B-site doping effects on magneto-transport of $RE_{0.55}Sr_{0.45}Mn_{1-x}Ru_xO_3$ manganites in the vicinity of the SGI and FMM border

H. S. Alagoz[1,*], I. Živković[2], S. T. Mahmud[1], M. M. Saber[1], G. Perrin[1,3], J. Shandro[1], M. Khan[1], Y. Zhang[1], M. Egilmez[4], J. Jung[1], and K. H. Chow[1]

[1] Department of Physics, University of Alberta, Edmonton, AB, T6G 2E1, Canada
[2] Institute of Physics, Bijenička 46, HR-10000 Zagreb, Croatia
[3] Polytech' Clermont-Ferrand, Université Blaise Pascal, 63000 Clermont-Ferrand, France
[4] Department of Materials Science and Metallurgy, University of Cambridge, Cambridge CB2 3QZ, United Kingdom

Received 2 April 2013, revised 6 June 2013, accepted 18 June 2013
Published online 23 July 2013

Keywords ferromagnetism, manganites, percolation loss, percolation onset, ruthenium

* Corresponding author: e-mail alagoz@ualberta.ca, Phone: +1 780 4924176, Fax: +1 780 4920714

Competing effects of the A-site and B-site doping on the magneto-transport have been investigated in $RE_{0.55}Sr_{0.45}Mn_{1-x}Ru_xO_3$ ($0 \le x \le 0.25$) manganites with RE (A-site) = Gd_ySm_{1-y} ($0 \le y \le 1$). The Ru (B-site)-free system is a ferromagnetic metal (FMM) for $y \le 0.5$ and a spin-glass insulator (SGI) for $y > 0.5$. For $y \le 0.5$, Ru improves the metallicity compared to the Ru-undoped system. For $y > 0.5$, Ru-doping induces a transition from the SGI to FMM state, above a percolation threshold which depends strongly on the A-site substitution. Interestingly, irrespective of the A-site doping level y, the percolation is suppressed when the Ru concentration x exceeds ~16% to 18%.

The observation of colossal magneto resistance (CMR) in hole doped perovskite manganites ABO_3 have important scientific and technological ramifications. This has motivated many studies aimed at understanding and manipulating their magneto-transport properties [1–3]. Strong correlations between spin, charge, and orbital degrees of freedom play important roles in the manganites, and phase competition/separation is particularly prominent for manganites with the composition $RE_{1-x}AE_xMnO_3$ (where RE and AE are the rare earth and alkaline elements, respectively) with $x \sim 0.5$. In this regard, one interesting system is $RE_{0.55}Sr_{0.45}MnO_3$. It is found [4] that by changing the RE from Gd to Sm, which therefore increases the averaged ionic radius of the A-site cations $\langle r_A \rangle$ (electronic bandwidth) and simultaneously decreases the amount of quenched disorder, the system evolves from a spin-glass insulator (SGI) to a ferromagnetic metal (FMM).

In manganites, it is well-established that substitution of Mn ions with another dopant, i.e., "B-site doping," can produce dramatic effects on the host's transport and magnetic properties. Among the many possible B-site dopants, Ru has been found to be particularly efficient at enhancing the ferromagnetic interactions and the metallicity of a number of manganites, resulting in significant enhancements of the material's Curie and metal-insulator temperatures T_C and T_{MIT}, respectively (see e.g., Refs. [5–8]). The interactions between Ru^{4+} ($t_{2g}^4e_g^0$), Ru^{5+} ($t_{2g}^3e_g^0$), Mn^{3+} ($t_{2g}^3e_g^1$), and Mn^{4+}($t_{2g}^3e_g^0$) can include FMM, FMI (ferromagnetic insulator), and AFMI (anti-ferromagnetic insulator), which have different effects on the magnetic and transport properties of the material. Hence the relative importance of these interactions governs the sample's metallicity and ferromagnetism at any particular Ru doping level. It is therefore worthwhile to systematically investigate and contrast the effects of Ru on manganites that are in the vicinity of the SGI and FMM border [4]. In particular, issues of interest include: *How does Ru enhance/suppress the T_C and T_{MIT} of the $RE_{0.55}Sr_{0.45}MnO_3$ systems as one tunes the RE composition across this border?*

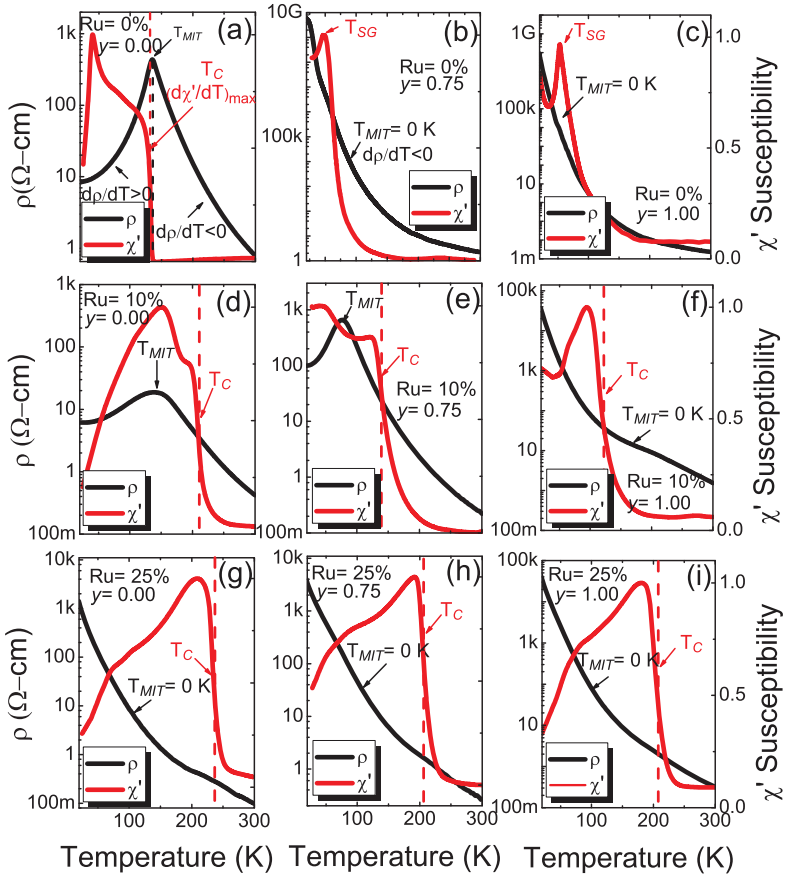

Figure 1 Temperature dependence of resistivity (ρ) and normalized ac susceptibility (χ') of $x = 0\%$, 10%, and 25% Ru doped $y = 0.00$, 0.75, and 1.00 compositions.

Which properties are governed entirely by the B-site (Ru) doping, and which ones are affected only by the A-site (RE) substitutions? As the Ru doping level within a series increases, how will the competing interactions due to its substitution manifest themselves in the metallicity and ferromagnetism of the system, e.g., are there any obvious regimes where one type of interaction dominates?

In this paper, we address these issues by synthesizing bulk samples of $RE_{0.55}Sr_{0.45}Mn_{1-x}Ru_xO_3$ with $RE = Gd_ySm_{1-y}$ ($0 \leq y \leq 1$) and Ru doping level x between 0 and 0.25. They have been chosen because of the properties of their undoped (no Ru) counterparts which depend on the average cation radius $\langle r_A \rangle$ (from 1.2121 Å for $y = 0$ to 1.1984 Å for $y = 1$). In particular, $Gd_{0.55}Sr_{0.45}MnO_3$ (i.e., $y = 1$) is a SGI; $(Gd_ySm_{1-y})_{0.55}Sr_{0.45}MnO_3$ with $y = 0.95$, 0.85, 0.75, 0.70, and 0.65 are near the border between SGI and FMM; and $(Gd_ySm_{1-y})_{0.55}Sr_{0.45}MnO_3$ with $y = 0.50$, 0.35, and 0 are further into the FMM regime.

The bulk (polycrystalline) samples were prepared via a standard solid state reaction method [6, 9].The temperature dependence of the resistivity measurements were carried out for rectangular bar-shaped samples in the absence of an applied field in the range 10–300 K in 2 K steps using a standard four point probe technique. The crystal structure and phase purity of the samples were studied by using powder X-ray diffraction performed on a Rigaku X-ray diffractometer with a rotating anode and Cu Kα radiation. In the resistivity measurements, the samples were first cooled down to ~10 K and then the resistance was measured during warming using a current of magnitude 1 μA. In samples where there is a clear metal-insulator transition, the T_{MIT} is defined as the temperature of the peak resistivity. Furthermore, T_{MIT} is assigned a value of zero if the sample is insulating. The temperature dependence of ac magnetic susceptibility was measured either in a home-built or a CryoBIND susceptometer. The samples were zero-field cooled and the measurements taken upon warming in an ac field of ~5 Oe at 2 kHz. The values of the Curie temperature T_C were estimated using the gradient method, i.e., defined by the most negative slope of the in-phase component (χ') of the ac magnetic susceptibility. In samples with a spin-glass transition, the transition temperature T_{SG} is defined to be the temperature of the peak in χ'. As indicated in the previous section, it is useful to have a parameter that provides a quantitative measure of the amount of the quenched disorder due to the different elements occupying the A-site. For this purpose, we use the average ionic radius of the A-site cations $\langle r_A \rangle = (1 - x)r_{RE}^{3+} + xr_{AE}^{2+}$ where x and r are the fractional occupancies and nine-coordinate ionic radii [10] of the RE and AE cations, respectively. The relevant values of r are $r_{Gd}^{3+} = 1.107$ Å, $r_{Sm}^{3+} = 1.132$ Å, and $r_{Sr}^{2+} = 1.32$ Å.

In Fig. 1a–i, we show the temperature dependence of the resistivity $\rho(T)$ and the in-phase component of the ac susceptibility $\chi'(T)$ of 0%, 10%, and 25% Ru doped $RE = Gd_ySm_{1-y}$ ($y = 0.00$, 0.75, and 1.00) compositions. Consider first the

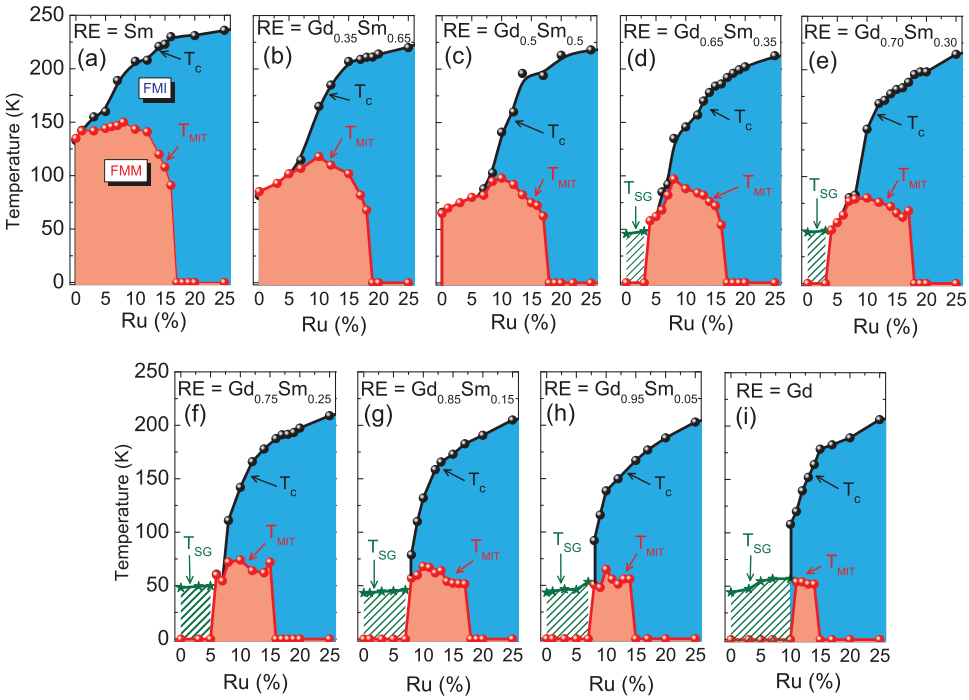

Figure 2 Magnetic phase diagram of $RE_{0.55}Sr_{0.45}Mn_{1-x}Ru_xO_3$ with $RE = Gd_ySm_{1-y}$ ($0 \leq y \leq 1$) and Ru doping level x between 0% and 25%. Red and blue areas are used as visual aids for identifying ferromagnetic metallic (FMM) and ferromagnetic insulating (FMI) regimes, respectively. Green dashed areas indicate the presence of spin-glass insulators (SGI).

Ru doped series for $y = 0.00$ in Fig. 1a, d, and g. SSMO ($y = 0.00$) with 0% Ru shows a metal to insulator transition at $T_{MIT} = 136$ K, and a transition from a ferromagnetic to a paramagnetic state at $T_C = 135$ K. The sharp peak in $\chi'(T)$ around 40 K has been interpreted as the onset of the antiferromagnetic ordering and/or spin reorientation of the spontaneous magnetization [11]. However, this peak has significantly diminished by 10% Ru doping (see Fig. 1d), where the sample shows a T_C of 204 K above the T_{MIT} of 140 K. At 25% Ru, the sample becomes fully insulating ($T_{MIT} = 0$ K); however, it also shows a ferromagnetic transition at $T_C = 230$ K (see Fig. 1g).

In the case of Ru-free $y = 0.75$ composition (see Fig. 1b), the cusp at ~48 K in the ac susceptibility is indicative of the spin-glass transition temperature (T_{SG}). Furthermore, this sample is also insulating throughout the entire temperature range studied. This is in contrast to the behavior of the $y = 0.75$, 10%, Ru sample (see Fig. 1e), which exhibits the FMM state with $T_C = 137$ K and $T_{MIT} = 77$ K. The presence of two phases with different chemical compositions could result in the double humps observed in the ac spectrum. For the 25% Ru doped $y = 0.75$ sample (see Fig. 1h) the $\chi'(T)$ shows that the ferromagnetism persists at temperatures up to $T_C = 204$ K, while the $\rho(T)$ shows that the sample is insulating at all temperatures.

Figure 1c, f, and i present $\rho(T)$ and $\chi'(T)$ dependences of Ru doped GSMO ($y = 1.00$) samples. The Ru-free sample shows a T_{SG} at 45 K with an insulating-like $\rho(T)$ behavior, indicating a spin-glass insulating phase. (This is in a good agreement with previous ac magnetic measurements obtained for this composition [12, 13].) At Ru 10%, where the sample is at the verge of the percolation onset, the $\chi'(T)$ shows a downturn towards the lowest temperature which is discernible at around 50 K. This could be related to the T_{SG} transition. Moreover, the compound undergoes a ferromagnetic transition with T_C at around 110 K. Finally, at 25% Ru doping level, the sample shows a ferromagnetic insulating phase with $T_{MIT} = 0$ K and $T_C = 210$ K.

Here, the clear downturn of $\chi'(T)$ as a function of decreasing temperature is observed in all 25% Ru doped compositions (see Fig. 1g–i). A similar decrease of the magnetization and/or in-phase ac susceptibility has been observed in B-site doped single crystal of $Gd_{0.6}Sr_{0.4}MnO_3$ manganites [14]. These transitions may be caused by the formation of the spin-glass phase. However, the nature of these transitions has not been studied in detail.

In the remainder of this paper, we focus on the "primary," i.e., the highest temperature, magnetic, and transport transitions in each sample. The dependence of T_C, T_{SG}, and T_{MIT} on Ru content for the nine different values of y are shown in Fig. 2. There are a number of notable features that can be inferred from these "phase diagrams", as detailed below: (i) Consider the Ru-free samples, i.e., $x = 0$. The undoped $RE = Sm$ ($y = 0$) sample has the largest average ionic radius $\langle r_A \rangle = 1.2121$ Å among all the samples studied and T_{MIT} of 135 K. T_{MIT} drops as $\langle r_A \rangle$ decreases, i.e., increasing y, and in $RE = Gd_{0.50}Sm_{0.50}$ ($y = 0.50$) its value has been reduced to 65 K. For $y > 0.5$, the undoped systems enter the SGI regime

(no T_{MIT}) with T_{SG} of ~50 K. These results are similar to those observed in single crystal $(Gd_ySm_{1-y})_{0.55}Sr_{0.45}MnO_3$ manganites [13]. (ii) For the $y \leq 0.5$ series, the undoped samples are ferromagnetic materials. Doping these compounds with Ru up to 10% gradually increases T_{MIT}. However, T_{MIT} decreases as the Ru doping level is increased further. (iii) For the $y > 0.5$ series, the undoped samples are spin-glass insulators. However, doping these samples with Ru always induces a transition from a SGI to a FMM phase at a certain doping level x_{po}. The value of x_{po} increases (from 3% to 10%) with an increasing y. (iv) In every series ($0 \leq y \leq 1$), T_{MIT} drops sharply to zero above a value of x_{po} = 16% to 18%, i.e., there is a transition from FMM to FMI at this doping level. (v) Consider the samples within a series that are in a FMM state, i.e., they show both a T_C and a T_{MIT}. In general, T_C increases with the Ru doping level. At low Ru concentrations, the T_C and T_{MIT} values are similar. However, there is a significant divergence between T_C and T_{MIT} at larger Ru doping levels, as is also seen in some other manganite systems [6, 8].

We now discuss possible explanations for the observations discussed above. Within each series, ferromagnetism eventually occurs as the Ru doping level increases even if the undoped samples are SGI. Furthermore, there is an overall increase in T_C with an increasing Ru concentration. These observations imply that increasing the Ru level produces enhancement of ferromagnetic interactions in all members of the series. In fact, it is well-accepted that substitution of Ru for Mn in manganites has the tendency to form ferromagnetic clusters around the Ru [15, 16].

At low Ru concentrations, the proposed mechanisms for the formation of the FM clusters rely most effectively on the Ru^{5+} which lead to an increase of the double exchange (DE) interactions for Mn–Mn and Ru–Mn ions. The Ru^{5+} not only reduces the Mn^{4+} but also generates the equivalent number of Mn^{3+} due to the $2Mn^{4+} \rightarrow Ru^{5+} + Mn^{3+}$ substitution reaction (see Ref. [8]). In a number of manganites near or at half-doping, an increase in the e_g electron density (i.e., Mn^{3+} content) via Ru doping has been suggested to increase the ferromagnetic interaction between Mn^{3+} and Mn^{4+} ions [7, 17, 18]. It is not clear if such a mechanism is valid for our systems since it is known that in $Sm_{0.55}Sr_{0.45}MnO_3$, T_C actually decreases with an increasing Mn^{3+} content, i.e., as the Sr content decreases in the vicinity of Sr = 0.45 [11, 19, 20]. This would suggest that the effective change in the Mn^{3+}/Mn^{4+} ratio caused by Ru substitution should suppress the ferromagnetic interaction and lead to a decrease in T_C, in contrast to our observations. However, caution should be exercised with regards to making a direct comparison between our Ru systems and that of Ru-undoped $Sm_{0.55}Sr_{0.45}MnO_3$ because changing the Sr content in the latter not only changes the e_g density but also other parameters such as $\langle r_A \rangle$ and the A-site quenched disorder (σ^2), which we are not directly doing as we substitute Ru for Mn within a particular series. Furthermore, in our systems, the existence of other magnetic interactions, such as those between $Mn^{3+}(t_{2g}^3 e_g^1)$ and Ru^{5+} $(t_{2g}^3 e_g^0)$ ions may also contribute to an increase in the DE interaction [21, 22] and hence the ferromagnetic transition temperature.

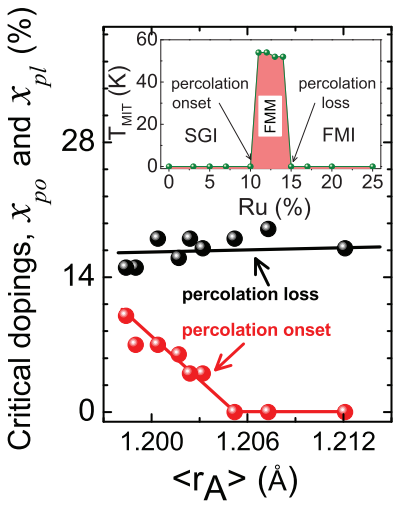

Figure 3 Dependence of x_{po} and x_{pl}, the Ru doping level at which the percolation onset and loss occur, on $\langle r_A \rangle$. Inset: An example of the dependence of T_{MIT} on x in $Gd_{0.55}Sr_{0.45}Mn_{1-x}Ru_xO_3$ ($y = 1$) system ($\langle r_A \rangle = 1.1984$ Å), showing both the percolation onset and loss. SGI, FMM, and FMI mark spin-glass insulator, ferromagnetic metal, and ferromagnetic insulator, respectively.

For $y \leq 0.5$, Ru increases metallicity (increases T_{MIT}) for x up to 10%. However, for $y > 0.5$, Ru does not generate any metallicity up to the critical concentration x_{po} at which the percolation takes place. This is summarized in Fig. 3 which shows the dependence of the "percolation onset" value x_{po} on the average ionic radius for all the series. This figure also highlights the fact that as $\langle r_A \rangle$ decreases (y increases), x_{po} must increase to induce the percolation onset. One possible explanation of these results is that at low Ru doping levels and large y, the Ru-induced FMM clusters are too small in size and do not percolate. x_{po} shows a strong ionic size dependence, i.e., it increases with an increasing y (or decreasing $\langle r_A \rangle$). The Ru-free system ($x = 0$) becomes more disordered with an increasing y. In this case, ferromagnetism is gradually suppressed due to a weakening of DE and subsequent reduction of the hopping ability of itinerant e_g electrons [18]. Consequently, the FMM clusters become more progressively disconnected from each other and the amount of insulating phase increases. In order to recover the metallicity in the system, doping with more Ru is required to increase the size of FMM clusters and hence induce the percolation/metallicity.

While one consequence of increasing Ru is to increase the ferromagnetism and metallicity within a series, as discussed above, other interactions involving Ru are also important and their relative importance determine the rich behavior observed in Figs. 2 and 3. At high doping levels, Ru predominantly exists in the 4+ oxidation state which depletes the hole concentrations (i.e., Mn^{4+} content) and also a significant number of hopping sites [22]. The Ru^{4+} ions are in a low spin state (i.e., $t_{2g}^4 e_g^0$), making it difficult to form the DE interaction between Mn^{3+} and Ru^{4+} ions [8]. However, the ferromagnetic superexchange (SE) interaction is possible

between the Mn^{3+} and Ru^{4+} ions. DE and SE interactions favor different transport properties: DE enhances metallicity while SE favors insulating behavior, leading to the possible coexistence of FMM and FMI phases/clusters in the sample [8]. This may explain the gradual decrease in T_{MIT}, associated with an increase of T_C, for Ru doping levels $x > 10\%$, i.e., although FM interactions continue to be important, the DE interaction becomes progressively "less dominant" than the SE interactions. Note, however, a previous study of the bilayered manganese oxide $La_{1.2}Sr_{1.8}(Mn_{1-y}Ru_y)_2O_7$ [23] has suggested that their observed increase of T_C with Ru doping is due to another mechanism: namely, the antiferromagnetic superexchange interaction between Ru and Mn moments. Hence, the nature of the exchange interactions between Ru and Mn is still a subject of controversy.

An intriguing feature is seen in Fig. 2 for x above approximately 16–18% in each series: a transition from FMM to FMI phase occurs, represented by a sharp suppression of the metallicity by Ru doping, i.e., T_{MIT} drops to zero. At this doping level x_{pl}, the percolation is lost. Interestingly, x_{po} is insensitive to the A-site substitution level y, and hence $\langle r_A \rangle$, as shown in Fig. 3. Therefore, the relevant mechanism that is responsible for the suppression of metallicity at a fixed x_{pl} should be independent of $\langle r_A \rangle$. SE interactions have previously been attributed to the suppression of metallicity in Ru doped manganites above $x = 0.20$ [8]. However, since x_{po} is very insensitive to y and hence the ionic radius $\langle r_A \rangle$, and SE depends strongly on $\langle r_A \rangle$ [24], SE interactions alone cannot account for this sharp suppression in our samples. It is important to note that the change of the $\langle r_A \rangle$ of A-site does not affect the number of Mn^{3+} and Mn^{4+} ions because we keep the oxidation states for A site ions (RE^{3+} and AE^{2+}) same. This fact alone may explain the indirect effect of the $\langle r_A \rangle$ (A-site doping) on suppression of the metallicity.

In summary, we investigated the effects of Ru substitution of the Mn-site (B-site doping) on the metallicity and ferromagnetism in $RE_{0.55}Sr_{0.45}MnO_3$ by choosing RE (A-site) = Gd_ySm_{1-y} $(0 \leq y \leq 1)$ such that the samples without Ru evolve from a SGI to a FMM. We have constructed "temperature versus x" phase diagrams of these $Gd_ySm_{1-y}Sr_{0.45}Mn_{1-x}Ru_xO_3$ manganites for $0 \leq x \leq 0.25$. They allowed us to distinguish the effects of the A-site (RE) doping from those due entirely to the B-site (Ru) doping. For $y \leq 0.5$, which are already ferromagnetic even in the absence of any Ru, increasing the Ru concentration enhances both the ferromagnetism and initially, the metallicity of each member of the series. On the other hand, for $y > 0.5$, the systems are SGI at low Ru doping level. However, they exhibit a transition to FMM at higher doping above a percolation threshold x_{po} whose value increases with an increasing y. Irrespective of the value of y, there is a transition from a FMM to a FMI phase at a critical doping x_{pl} of approximately 16–18%.

Acknowledgement This work was supported by the Natural Sciences and Engineering Research Council of Canada. S.T.M. is partially supported by Alberta Innovates-Technology Futures and Alberta Advanced Education and Technology.

References

[1] Y. Tokura, Rep. Prog. Phys. **69**, 797 (2006).
[2] E. Dagotto, Nanoscale Phase Separation and Colossal Magnetoresistance (Springer, Berlin, 2003).
[3] M. Egilmez, K. H. Chow, and J. A. Jung, Mod. Phys. Lett. B **25**, 697 (2011);
M. Egilmez, M. M. Saber, I. Fan, K. H. Chow, and J. Jung, Phys. Rev. B **78**, 172405 (2008);
S. T. Mahmud, M. M. Saber, H. S. Alagoz, K. Biggart, R. Bouveyron, Mahmud Khan, J. Jung, and K. H. Chow, Appl. Phys. Lett. **100**, 2320406 (2012);
S. T. Mahmud, M. M. Saber, H. S. Alagoz, R. Bouveyron, J. Jung, and K. H. Chow, Appl. Phys. Lett. **100**, 072404 (2012).
[4] Y. Tomioka and Y. Tokura, Phys. Rev. B **70**, 014432 (2004).
[5] R. K. Sahu, S. S. Manoharan, Q. Mohammad, M. L. Rao, and A. K. Nigam, J. Appl. Phys. **91**, 7724 (2002);
R. K. Sahu, Q. Mohammad, M. L. Rao, S. S. Manoharan, and A. K. Nigam, Appl. Phys. Lett. **80**, 88 (2002).
[6] M. M. Saber, M. Egilmez, A. I. Mansour, I. Fan, K. H. Chow, and J. Jung, Phys. Rev. B **82**, 88 (2010).
[7] C. Martin, A. Maignan, M. Hervieu, C. Autret, B. Raveau, and D. I. Khomskii, Phys. Rev. B **63**, 174402 (2001).
[8] Y. Ying, J. Fan, L. Pi, Z. Qu, W. Wang, B. Hong, S. Tan, and Y. Zhang, Phys. Rev. B **74**, 144433 (2006).
[9] M. Egilmez, I. Isaac, D. D. Lawrie, K. H. Chow, and J. Jung, J. Mater. Chem. **18**, 5796–5801 (2008).
[10] R. D. Shannon, Acta Crystallogr. **32**, 751 (1976).
[11] V. Y. Ivanov, A. A. Mukhin, A. S. Prokhorov, and A. M. Balbashov, Phys. Status Solidi B **236**, 445 (2003).
[12] M. Egilmez, K. H. Chow, and J. Jung, Appl. Phys. Lett. **89**, 062511 (2006).
[13] Y. Tomioka, Y. Okimoto, J. H. Jung, R. Kumai, and Y. Tokura, Phys. Rev. B **68**, 094417 (2003).
[14] H. Sakai, K. Ito, T. Nishiyama, X. Yu, Y. Matsui, S. Miyasaka, and Y. Tokura, J. Phys. Soc. Jpn. **77**, 124712 (2008).
[15] C. Martin, A. Maignan, M. Hervieu, B. Raveau, and J. Hejtmanek, Eur. Phys. J. **16**, 469 (2000).
[16] I. Dhiman, A. Das, A. K. Nigam, and U. Gasser, J. Phys.: Condens. Matter **23**, 246006 (2011).
[17] C. Krishnamoorthi, S. K. Barik, and R. Mahendiran, Solid State Commun. **151**, 107–111 (2011).
[18] C. L. Lu, X. Chen, S. Dong, K. F. Wang, H. L. Cai, J. -M. Liu, D. Li, and Z. D. Zhang, Phys. Rev. B **79**, 245105 (2009).
[19] Y. Tomioka, H. Hiraka, Y. Endoh, and Y. Tokura, Phys. Rev. B **74**, 104420 (2006).
[20] A. Maignan, C. Martin, M. Hervieu, B. Raveau, and J. Hejtmanek, J. Appl. Phys. **89**, 4 (2001).
[21] C. Zener, Phys. Rev. **82**, 403 (1951).
[22] R. K. Sahu and S. S. Manoharan, J. Appl. Phys. **91**, 10 (2002).
R. K. Sahu, M. L. Rao, S. S. Manoharan, K. Dörr, and K.-H. Müller, Solid Satate Commun. **123**, 217–222 (2002).
[23] Y. Onose, J. P. He, Y. Kaneko, T. Arima, and T. Tokura, Appl. Phys. Lett. **86**, 242502 (2005).
[24] J. S. Zhou and J. B. Goodenough, Phys. Rev. Lett. **96**, 247202 (2006).